Dual spindle formation in zygotes keeps parental genomes apart in early mammalian embryos

Judith Reichmann[1], Bianca Nijmeijer[1], M. Julius Hossain[1], Manuel Eguren[1], Isabell Schneider[1], Antonio Z. Politi[1], Maria J. Roberti[1], Lars Hufnagel[1], Takashi Hiiragi[2] and Jan Ellenberg[1]*

[1]Cell Biology and Biophysics Unit, European Molecular Biology Laboratory, Meyerhofstrasse 1, 69117 Heidelberg, Germany.

[2]Developmental Biology Unit, European Molecular Biology Laboratory, Meyerhofstrasse 1, 69117 Heidelberg, Germany.

*Corresponding author. E-mail: jan.ellenberg@embl.de

Abstract: At the beginning of mammalian life the genetic material from each parent is replicated in a separate pronucleus and meets for the first time when the fertilized egg divides. So far, it was thought that a single microtubule spindle is responsible to spatially combine the two genomes and then segregate them to create the two-cell embryo. Utilising the high spatio-temporal resolution of light-sheet microscopy, we show that two separate bipolar spindles form in the zygote, that independently congress and segregate the maternal and paternal genomes. These two spindles normally align their poles prior to anaphase but keep the parental genomes apart during the first embryonic division. This spindle assembly mechanism provides a rationale for the high frequency of erroneous divisions into more than two blastomeric nuclei observed in mammalian zygotes and reveals the mechanism behind the long-standing observation that parental genomes occupy separate nuclear compartments in the two-cell embryo.

After fertilization, the haploid genomes of egg and sperm have to come together to form the genome of a new diploid organism, a moment that is of fundamental biological importance. In mammals, parental chromosomes are first replicated in two separate pronuclei and meet for the first time upon entry into the first zygotic mitosis after the nuclear envelopes break down. Based on analysis in fixed embryos and low resolution live imaging, it was so far assumed that a single bipolar microtubule system assembles around both parental genomes (Fitzharris 2009, Courtois,

Schuh et al. 2012, Coelho, Bury et al. 2013) that jointly congresses and biorients both sets of parental chromosomes, similar to the self-assembly of one large bipolar system that occurs in mammalian oocytes (Schuh and Ellenberg 2007, Kitajima, Ohsugi et al. 2011, Holubcova, Blayney et al. 2015). However, due to the extreme light-sensitivity of the mammalian embryo, previous studies could not capture the details of the dynamic process of zygotic spindle assembly. Given its key role for our understanding of the cell division mechanisms that operate at the beginning of mammalian life, we investigated zygotic spindle assembly and joining of the parental genomes using our recently developed inverted light sheet microscope, which allows fast and high resolution 3D time-lapse imaging of early embryonic development due to its low phototoxicity and rapid image acquisition (Strnad, Gunther et al. 2016).

To examine precisely how the parental genomes join for the first time, we imaged live embryos in which the maternal and paternal centromeres were differentially fluorescently labelled (Miyanari, Ziegler-Birling et al. 2013). This revealed that the two genomes remained spatially separate throughout the first mitosis including chromosome segregation (Supplementary Fig. 1, Supplementary Movie 1).To understand why the genomes are not mixed, we next imaged the process of spindle assembly using fluorescently labelled MTOCs and spindle microtubules with high spatio-temporal resolution (Fig. 1A, Supplementary Movie 2). Surprisingly, we found that cytoplasmic microtubule asters accumulate around each pronucleus and self-organize into two separate bipolar spindles after nuclear envelope breakdown (Fig. 1A). Subsequently, the two spindles align and come into close apposition to form one compound and roughly barrel-shaped system. This compound spindle typically had two clusters of MTOCs at at least one of its poles suggesting that the two spindles align closely but do not merge into one functional unit even in anaphase (Fig. 1A,B arrowheads, Supplementary Movie 2). To ensure that the formation of two separate spindles was not induced by imaging conditions or the fluorescent markers, we performed high resolution 3D immunofluorescence analysis of zygotes visualizing endogenous spindle poles, microtubules, kinetochores and DNA. This clearly showed that in early and mid prometaphase, two separate bipolar spindles are also formed in untreated embryos (Fig. 1B).

To characterize the different steps of this unusual dual spindle assembly, we imaged maternal and paternal centromeres in relation to growing spindle microtubule tips in live zygotes. This

allowed us to define three phases of zygotic spindle assembly (Fig. 2A). A transient first phase (~3 min; 10.3 ± 3.5 min to 13. 4 ±4 min after NEBD), characterized by the clustering of cytoplasmic microtubule asters around the two pronuclei; followed by phase 2 (~16 min; 14.5± 4 min to 30.7 ± 6.5 min after NEBD), where individual bipolar spindles assemble around each parental genome; and subsequently phase 3 (~83 min; 46.7±17 min to 129.2 ± 16.5 min after NEBD), when the two spindles align and combine into a compound barrel shaped structure.

To test if the two zygotic spindles are functionally independent, we measured the timing and direction of maternal and paternal chromosome congression (Supplementary Fig. 2A, B and Fig. 2A, B; for details see methods). Maternal and paternal chromosomes already congressed during phase 2 of the assembly process, while the spindles were clearly separated (Supplementary Fig. 2A, B). Parental chromosome congression was not correlated in time until shortly before anaphase, suggesting that they are moved by different microtubule systems (Supplementary Fig. 2C). Furthermore, the parental genomes were congressed in different directions along separate spindle axes, as evidenced by the large difference between the angles of the two forming metaphase plates, which became parallel only later during dual spindle alignment in phase 3 (Fig. 2B-D; Supplementary Fig. 2D, E). Furthermore, tracking of growing microtubule tips also showed two different directions of microtubule flow during phase 2 (Supplementary Fig. 3A, B, Supplementary Movies 3, 4). This independent congression frequently led to an offset in the final bioriented position of the paternal and maternal metaphase plates at the end of phase 3 prior to and during segregation (Fig. 2A arrows). Together, this data shows that each of the two spindles around the parental genomes is independently functional for chromosome congression and that they apparently also function uncoupled from each other in chromosome segregation.

This surprising assembly of two independent spindles led us to hypothesize that a failure to align the parental spindles at one or both poles might underlie the high frequency of erroneous zygotic divisions into embryos with blastomeres containing two nuclei, or even three or four celled embryos that have been observed in IVF clinics (Kligman, Benadiva et al. 1996, Balakier and Cadesky 1997, Meriano, Clark et al. 2004, Egashira, Yamauchi et al. 2015, Kalatova, Jesenska et al. 2015). In order to test this hypothesis, we increased the distance between the two pronuclei by transient treatment with the microtubule depolymerizing drug nocodazole, which led to a larger

gap between the two self-assembling spindles (Fig. 3, Supplementary Movies 5-7). Indeed, such embryos frequently failed to fully align the parental spindles at one or both poles. However, this did not delay anaphase but resulted in chromosome segregation by two spindles in different directions, leading to two cell embryos with one or two bi-nucleated blastomeres (Fig. 3, Supplementary Movies 6-7)). By contrast, embryos that did align the two spindles parallel to each other before anaphase cleaved into two blastomeres with single nuclei as expected (Supplementary Movie 5). This data shows that failure to align the two zygotic spindles does not delay anaphase and gives rise to multinucleated two-cell embryos that phenocopy frequently observed errors in human embryonic development in IVF clinics.

Our new finding of dual spindle assembly in the mammalian zygote would also offer a mechanistic explanation for the long-standing observation that the parental genomes occupy separate compartments inside the nuclei of two- and four-cell embryo blastomeres (Mayer, Niveleau et al. 2000, Mayer, Smith et al. 2000). If dual spindle assembly around two pronuclei was responsible for genome compartmentalization in the two-cell embryo, paternal genomes should mix in subsequent divisions, where only one nucleus is present per cell. To test this, we imaged the metaphase plate of live hybrid mouse embryos from the zygote to the 8-cell stage and quantified the separation of maternal and paternal centromeres. As predicted, the parental genomes had only a very small degree of overlap in zygotes, but became rapidly mixed in the subsequent developmental stages (Supplementary Fig. 4A-D). This rapid loss of genome compartmentalization was also seen in in vivo developed isogenic embryos, where we labelled the paternal genome with the thymidine analogue EdU (5-Ethynyl-2´-deoxyuridine) (Supplementary Fig. 4E-I). This data suggests that parental genomes are kept separate by two spindles only during the first mitosis but then mix during subsequent divisions driven by a single common spindle.

If dual spindle assembly is the mechanism for paternal genome compartmentalization (Supplementary Fig.5A), forcing the formation of a single spindle around both genomes in the zygote should mix them already in the first division. To test this prediction, we redirected spindle assembly with two small molecule inhibitors of microtubules and the motor protein Eg5. We transiently treated zygotes with Monastrol, which collected both genomes in a single microtubule

aster, and then allowed one bipolar spindle to form around both genomes after transiently depolymerising microtubules with Nocodazole (Supplementary Fig. 5B and 6, from here on referred to as MoNoc treated zygotes). MoNoc treated embryos captured and congressed chromosomes within a single spindle and showed a high degree of parental genome mixing in the first mitotic metaphase approaching a random arrangement (Fig. 4). This was significantly different from untreated or control zygotes in which the order of drug treatments is reversed (NocMo treated zygotes), which maintains dual spindle formation (Fig. 4; Supplementary Fig. 5C and 6). These data show that dual spindle formation in the zygote is responsible for parental genome separation in mammals.

Having an experimental method to induce mixing of the parental genomes in the zygote, put us in a position to test the hypothesis that nuclear compartmentalization plays a role in resolving epigenetic asymmetry in early development as proposed previously (Mayer, Smith et al. 2000, Probst and Almouzni 2008, Duffie and Bourc'his 2013, De La Fuente, Baumann et al. 2015). Independent of whether the parental genomes were experimentally mixed or allowed to stay separate, we found no difference in the total amount or the timing of equilibration for four different parent-specific epigenetic modifications (Supplementary Figs. 7, 8). We therefore conclude that early developmental epigenetic asymmetry is chromosome intrinsic and does not require parental genomes to occupy separate nuclear compartments.

In summary, we show here that two spindles form around pronuclei in mammalian zygotes which individually collect the parental genomes and then position them next to each other prior to the first anaphase. Our data explains for the first time how parental genome separation is achieved in mammalian embryos. To date, the formation of physically distinct mitotic spindles around the two pronuclei has been thought to be specific to certain arthropod species (Kawamura 2001, Snook, Hosken et al. 2011). Our finding that this occurs also in mammals, suggests that two zygotic spindles might be characteristic for many species that maintain separate pronuclei during the first round of DNA replication after fertilization. The alignment of the two spindles likely depends on the microtubule motor dynein, which can move *in vitro* assembled spindles together in *Xenopus* egg extracts (Gatlin, Matov et al. 2009) and is known to be required for normal zygotic spindle assembly in mouse (Courtois, Schuh et al. 2012).

We demonstrate that failure to align the two spindles produces errors in the zygotic division that closely resemble clinical phenotypes of human embryos in IVF procedures, suggesting that a similar mechanism of dual zygotic spindle assembly also occurs in human. This view is supported by the topological separation of parental chromosomes reported in human zygotes (van de Werken, van der Heijden et al. 2014) and by reports of aberrant zygotic divisions into three or four blastomeres or bi-nucleated blastomeres in human and cattle (Kligman, Benadiva et al. 1996, Balakier and Cadesky 1997, Meriano, Clark et al. 2004, Egashira, Yamauchi et al. 2015, Kalatova, Jesenska et al. 2015, Destouni, Zamani Esteki et al. 2016) . These severe and relatively frequent zygotic division errors in human and agriculturally used mammals thus find their likely mechanistic explanation in a failure of the close alignment of the two zygotic spindles prior to anaphase.

Beyond the new fundamental biological insight, if a similar mechanism indeed occurs in human zygotes is also of importance from an ethical perspective, as the merging of the two nuclei after fertilization defines the beginning of embryonic life as protected by law in several countries (e.g. Germany: Embryonenschutzgesetz (ESchG) § 8 Abs. 1).

Material and Methods

Mouse strains and embryo culture.

Mouse embryos were collected from superovulated 8- to 24-week-old female mice according to the guidelines of EMBL Laboratory Animal Resources and cultured in 30-µl drops of G1 (Vitrolife) covered by mineral oil (Ovoil, Vitrolife). Embryos used for immunofluorescence were isolated from C57BL/6J x C3H/He F1 females, or EGFP-Tuba C57BL/6J x C3H/He F1 females, mated with C57BL/6J x C3H/He F1 males and fixed at different stages of zygotic mitosis. Embryos used for imaging of parental chromosomes were isolated from C57BL/6J x C3H/He F1 or H2BmCherry C57BL/6J x C3H/He F1 females mated with Mus Spretus males (*Mus musculus* (MMU) and *Mus spretus* (MSP) hybrid embryo). Culture during imaging was performed as described (Strnad, Gunther et al. 2016) with minor modifications. In brief embryos were imaged

in G1 medium covered with mineral oil with 5% CO_2 and 5% O_2 atmosphere. To achieve mixing of chromosomes embryos were cultured with 0.1 mM Monastrol for 5 hours followed by 0.01mM Nocodazole for 1 hour. Subsequently embryos were imaged or allowed to develop until the two cell stage and then synchronised with 0.01mM Nocodazole or 0.1mM Monastrol and then fixed. For controls the order of drug treatment was reversed in addition to a no drug treatment control.

Expression Constructs and mRNA Synthesis

Constructs used for mRNA synthesis were previously described: TALE-mClover (pTALYM3B15 Addgene plasmid 47878) (Burton and Torres-Padilla 2010), EB3-mEGFP (Schuh and Ellenberg 2007), tdEos-Cep192 (Clift and Schuh 2015) (a kind gift from Melina Schuh). To generate EB3-mCherry full length Homo sapiens EB3 cDNA (NM_001303050.1, a generous gift from Niels Galjart) was tagged at the C-terminus with a tandem mCherry and cloned into the vector pGEMHE for mRNA production. To generate TALE-tdiRFP670, mRuby from pTALYM4SpiMi-01 (Miyanari, Ziegler-Birling et al. 2013)(Addgene plasmid 47879) was replaced with tdiRFP670 (Addgene plasmid 45466, the tandem construct was a kind gift from Pierre *Neveu*). After linearization of the template with PacI, capped mRNA was synthesized using T7 polymerase (mMessage mMachine Ultra Kit, following manufacturer's instructions, Ambion) and dissolved in 11 µl water. mRNA concentrations were determined using a NanoDrop (Thermo Fisher Scientific).

Immunofluorescence

For imaging of the mitotic spindle embryos were fixed and extracted as described (Kitajima, Ohsugi et al. 2011). Embryos were blocked in 5% normal goat serum, 3% BSA in PBST (0.1% Trition X-100) and then incubated overnight in blocking solution at 4 °C at the following antibody dilutions:1:500 mouse anti-tubulin (Sigma T6199) to visualise microtubules, 1:500 rabbit anti-pericentrin (Abcam ab4448) for staining of MTOCs, 1:100 human anti-Crest (Europe Bioproducts CS1058) to stain centromeres. Embryos were washed 3x 5 minutes with 0.3% BSA in PBST then incubated with anti-mouse Alexa 488, anti-rabbit Alexa 546, anti-human Alexa 647 all 1:500 in 5% normal goat serum, 3% BSA in PBST (all (Thermo Fisher Scientific

A11029, A11035, A21445 respectively) and 5ug/ml Hoechst33342 (Sigma) for 1 hour at room temperature. Embryos were washed with 0.3% BSA in PBST for 3x 5 minutes before imaging. For imaging of 5mC and 5hmC embryos were fixed for 20 minutes with 4% PFA in PBS. Embryos were washed 3 times in 1% BSA in PBS then extracted overnight in 1% BSA in PBS containing 0.5% Trition X-100 . Embryos were incubated for 1 hour at 37 °C in the presence of 10 µg/ml RNAse A (Sigma). Chromosomes were denatured by incubating the embryos in 4N HCL for 30 minutes at 37°C followed by neutralisation with 100mM Tris buffer (pH8) at room temperature. Embryos were blocked with 3% BSA and 5% normal goat serum in PBST and then incubated at 4C overnight with 1:3000 mouse anti 5-methylcytosine (Diagenode C152000081) and 1:3000 rabbit anti 5-hydroxymethylcytosine (RevMab Biosciences 31-1111-00). Embryos were washed with 3% BSA in PBST for 3x 5 minutes then incubated with 1:1500 anti-rabbit Alexa 647 (Thermo Fisher Scientific A21245), 1:1500 anti-mouse Alexa 546 (Thermo Fisher Scientific A11030) and 100nM Yoyo-1 (Thermo Fisher Scientific Y3601) for 1 hour at room temperature. Embryos were then washed 3x for 5 minutes with 3% BSA in PBST and imaged.

Micromanipulation

Embryos were injected based on methods described previously (Schuh and Ellenberg 2007) The injected volumes ranged between 10–15 pl (3%–5% of the embryo volume) of 0.125 – 0.3 µg/µl mRNA. mRNA-injected embryos were incubated at 37°C for 4–6 hr in G1 medium as described above to allow recombinant protein expression. For labelling of MTOCs and microtubule tips MMU zygotes were injected with mRNA encoding tdEos-Cep192 and EB3-mCherry. For differential labelling of maternal and paternal centromeres MMU x MSP embryos were injected with mRNA encoding fluorescent proteins fused to TALEs specific to the different centromeric satellite repeats as described previously (Miyanari, Ziegler-Birling et al. 2013).

Embryo Imaging

Time-lapse image acquisitions were performed using a previously described in-house-built inverted light-sheet microscope (Strnad, Gunther et al. 2016) with the following modifications: (i) Image acquisition was performed with an Orca Flash 4 V2 camera from Hamamatsu Photonics, Japan. (ii) A ZYNQ-based cRIO-9064 embedded controller from National Instruments was used for realtime control of all microscope components. (iii) A rotating 6mm thick and 25mm diameter glass plate (Thorlabs) was inserted in the illumination path between the objective lens and the tube lens to translate the beam in the back focal plane of the illumination objective lens. For imaging MTOCs and microtubules stacks of 101 images with 520nm between planes were acquired simultaneously for mCherry and EGFP signals at 45 sec time intervals. Fixed embryos stained for spindle components and epigenetic marks were imaged on a SP8 Leica confocal microscope equipped with a 63× C-Apochromat 1.2 NA water immersion objective lens. Images of embryos stained for spindle components or epigenetic marks were acquired at 90nm XY and 360nm Z.

Image processing and analysis

Images of embryos stained and fixed for spindle markers were deconvolved using the Huygens remote manger (Scientific Volume Imaging) and maximum intensity projected in Arivis (arivis Vision4D). Time-lapse images were processed for extraction of raw camera data as described (Strnad, Gunther et al. 2016). Time-lapse movies were generated as described (Strnad, Gunther et al. 2016) or exported from Arivis. Phases of zygotic mitosis were scored manually according to spindle morphology and presence of two bi-polar or single barrel shaped spindle. Spindles were segmented using an Arivis inbuilt intensity threshold filter. Chromosomes were segmented using an in house developed MATLAB segmentation pipeline based on intensity threshold and connected component analysis. Shape and direction of chromosomes are represented using Eigen value and Eigen vector of the segmented chromosomes in order to measure chromosome congression and the angle between parental chromosomes. Segmentation of 5mC and 5hmC signals was performed using a script developed in MATLAB that quantifies the distribution of the signals and their correlation using bright pixels. Segmentation of maternal and paternal centromeres was performed using an in house developed MATLAB segmentation pipeline and the mixing between parental centromeres was measured using the overlap between their 3D convex hulls. More details in Supplemental Material and methods

Acknowledgments

We thank Nathalie Daigle for cloning of the EB3-mCherry plasmid. We thank Pierre Neveu and Melina Schuh kindly providing tdiRFP670 and tdEos-Cep192, respectively. We thank Niels Galjart for kindly providing full length Homo sapiens EB3 cDNA (NM_001303050.1). We thank EMBL's laboratory of animal resources for excellent support with mouse strains. We thank Petr Strnad for development and assistance of the inverted light sheet microscope. The EMBL Advanced Light Microscopy Facility is acknowledged for support in image acquisition and analysis. We thank Arivis for support in image analysis. We thank James Reddington and Stephanie Alexander for critical reading of the manuscript. This work was supported by funds from the European Research Council (ERC Advanced Grant "Corema", grant agreement 694236) to J.E. and by the European Molecular Biology laboratory (all authors). J.R. was further supported by the EMBL Interdisciplinary Postdoc Programme (EIPOD) under Marie Curie Actions COFUND; M.E. by the EMBO long-term postdoctoral fellowship and EC Marie Slodowska-Curie postdoctoral fellowship; I.S. by a Boehringer Ingelheim Fonds Phd fellowship, M.J.R. by a Humboldt Foundation postdoctoral fellowship.

Author Contributions

J.E. and J.R. conceived the project and designed the experiments. J.R., B.N., M.E. and I.S. performed the experiments. M.J.R. supported the mouse EDU experiments. J.R., J.H. and A.P. analysed the data. T.H. and L.H. contributed to conception and design of the work. J.E. and J.R. wrote the manuscript. All authors contributed to the interpretation of the data and read and approved the final manuscript.

Competing financial interest

L.H. and J.E. are scientific co-founders and advisors of Luxendo GmbH (part of Bruker), that makes light sheet–based microscopes commercially available.

References

Balakier, H. and K. Cadesky (1997). "The frequency and developmental capability of human embryos containing multinucleated blastomeres." Hum Reprod **12**(4): 800-804.
Burton, A. and M. E. Torres-Padilla (2010). "Epigenetic reprogramming and development: a unique heterochromatin organization in the preimplantation mouse embryo." Brief Funct Genomics **9**(5-6): 444-454.
Clift, D. and M. Schuh (2015). "A three-step MTOC fragmentation mechanism facilitates bipolar spindle assembly in mouse oocytes." Nat Commun **6**: 7217.
Coelho, P. A., L. Bury, B. Sharif, M. G. Riparbelli, J. Fu, G. Callaini, D. M. Glover and M. Zernicka-Goetz (2013). "Spindle formation in the mouse embryo requires Plk4 in the absence of centrioles." Dev Cell **27**(5): 586-597.
Courtois, A., M. Schuh, J. Ellenberg and T. Hiiragi (2012). "The transition from meiotic to mitotic spindle assembly is gradual during early mammalian development." J Cell Biol **198**(3): 357-370.
De La Fuente, R., C. Baumann and M. M. Viveiros (2015). "ATRX contributes to epigenetic asymmetry and silencing of major satellite transcripts in the maternal genome of the mouse embryo." Development **142**(10): 1806-1817.
Destouni, A., M. Zamani Esteki, M. Catteeuw, O. Tsuiko, E. Dimitriadou, K. Smits, A. Kurg, A. Salumets, A. Van Soom, T. Voet and J. R. Vermeesch (2016). "Zygotes segregate entire parental genomes in distinct blastomere lineages causing cleavage-stage chimerism and mixoploidy." Genome Res **26**(5): 567-578.
Duffie, R. and D. Bourc'his (2013). "Parental epigenetic asymmetry in mammals." Curr Top Dev Biol **104**: 293-328.
Egashira, A., N. Yamauchi, K. Tanaka, C. Mine, H. Otsubo, M. Murakami, M. R. Islam, M. Ohtsuka, N. Yoshioka and T. Kuramoto (2015). "Developmental capacity and implantation potential of the embryos with multinucleated blastomeres." J Reprod Dev **61**(6): 595-600.
Fitzharris, G. (2009). "A shift from kinesin 5-dependent metaphase spindle function during preimplantation development in mouse." Development **136**(12): 2111-2119.
Gatlin, J. C., A. Matov, A. C. Groen, D. J. Needleman, T. J. Maresca, G. Danuser, T. J. Mitchison and E. D. Salmon (2009). "Spindle fusion requires dynein-mediated sliding of oppositely oriented microtubules." Curr Biol **19**(4): 287-296.
Holubcova, Z., M. Blayney, K. Elder and M. Schuh (2015). "Human oocytes. Error-prone chromosome-mediated spindle assembly favors chromosome segregation defects in human oocytes." Science **348**(6239): 1143-1147.
Kalatova, B., R. Jesenska, D. Hlinka and M. Dudas (2015). "Tripolar mitosis in human cells and embryos: occurrence, pathophysiology and medical implications." Acta Histochem **117**(1): 111-125.
Kawamura, N. (2001). "Fertilization and the first cleavage mitosis in insects." Dev Growth Differ **43**(4): 343-349.
Kitajima, T. S., M. Ohsugi and J. Ellenberg (2011). "Complete kinetochore tracking reveals error-prone homologous chromosome biorientation in mammalian oocytes." Cell **146**(4): 568-581.
Kligman, I., C. Benadiva, M. Alikani and S. Munne (1996). "The presence of multinucleated blastomeres in human embryos is correlated with chromosomal abnormalities." Hum Reprod **11**(7): 1492-1498.
Mayer, W., A. Niveleau, J. Walter, R. Fundele and T. Haaf (2000). "Demethylation of the zygotic paternal genome." Nature **403**(6769): 501-502.
Mayer, W., A. Smith, R. Fundele and T. Haaf (2000). "Spatial separation of parental genomes in preimplantation mouse embryos." J Cell Biol **148**(4): 629-634.
Meriano, J., C. Clark, K. Cadesky and C. A. Laskin (2004). "Binucleated and micronucleated blastomeres in embryos derived from human assisted reproduction cycles." Reprod Biomed Online **9**(5): 511-520.
Miyanari, Y., C. Ziegler-Birling and M. E. Torres-Padilla (2013). "Live visualization of chromatin dynamics with fluorescent TALEs." Nat Struct Mol Biol **20**(11): 1321-1324.
Probst, A. V. and G. Almouzni (2008). "Pericentric heterochromatin: dynamic organization during early development in mammals." Differentiation **76**(1): 15-23.
Schuh, M. and J. Ellenberg (2007). "Self-organization of MTOCs replaces centrosome function during acentrosomal spindle assembly in live mouse oocytes." Cell **130**(3): 484-498.
Snook, R. R., D. J. Hosken and T. L. Karr (2011). "The biology and evolution of polyspermy: insights from cellular and functional studies of sperm and centrosomal behavior in the fertilized egg." Reproduction **142**(6): 779-792.
Strnad, P., S. Gunther, J. Reichmann, U. Krzic, B. Balazs, G. de Medeiros, N. Norlin, T. Hiiragi, L. Hufnagel and J. Ellenberg (2016). "Inverted light-sheet microscope for imaging mouse pre-implantation development." Nat Methods **13**(2): 139-142.

van de Werken, C., G. W. van der Heijden, C. Eleveld, M. Teeuwssen, M. Albert, W. M. Baarends, J. S. Laven, A. H. Peters and E. B. Baart (2014). "Paternal heterochromatin formation in human embryos is H3K9/HP1 directed and primed by sperm-derived histone modifications." Nat Commun **5**: 5868.

Figure legends

Figures

Figure 1. Microtubule balls formed around each pro-nucleus after NEBD mature into individual bi-polar spindles followed by their fusion into a barrel-shaped spindle. (A) Live cell time-lapse-imaging of Mus Musculus x Mus Musculus (MMU x MMU) zygotes expressing EB3-mCherry (green) and tdEos-Cep192 (magenta). Dashed ellipsoids trace spindle outline. Scale bar, 10 µm. In 11 out of 13 analysed zygotes both or at least one of the dual spindle poles remained clearly split also after the spindles had parallelised. (B) Immunofluorescence staining of (MMU x MMU) mouse zygotes fixed at consecutive stages of development. Shown are z-projected images of confocal sections of zygotes at prophase; early pro-metaphase, late pro-metaphase, early metaphase; late metaphase and anaphase. Microtubules (green), Pericentrin (magenta), Crest (grey), and DNA (blue) are shown. Scale bar, 5 µm. White arrows indicate poles (A, B).

Figure 2. Spindle assembly and chromosome dynamics in the zygote are defined by three different phases. (A) Live cell time-lapse-imaging of Mus Musculus x Mus Spretus (MMU x MSPS)zygotes expressing fluorescent TALEs to label maternal (magenta) and paternal (cyan) chromosomes and EB3-mCherry (white). Phase 1 (blue): Microtubule ball formation around pronuclei. Phase 2 (red): Bi-polarisation of maternal and paternal spindle. Phase 3 (green): Formation of single barrel shaped spindle. Lower row, segmentation of paternal (cyan) and maternal (magenta) spindles in Phase 1 and Phase 2 and single bipolar spindle in Phase 3 (grey). Offset between maternal and paternal chromosomes at metaphase and anaphase is indicated with white arrows.(B) Schematic of measurements. (C,D) Angle between maternal and paternal chromosome axis over time for a single embryo (C) and averaged for 12 embryos (D) are shown. Phase 1, blue; Phase 2, red; Phase 3, green.

Figure 3: Proximity dependency of bipolar spindle fusion. (A) Live-cell time-lapse imaging of MMU x MMU mouse pre-implantation embryos expressing H2B-mCherry (magenta) and αTubulin-EGFP (green). Spindle morphology in pro-metaphase and anaphase in 3 representative zygotes treated with Nocodazole for > 10 hours. Representative z-projected images of a pro-metaphase and anaphase time point are shown for 3 different embryos. Arrowheads and PB indicate nuclei and polar body, respectively. Scale bar, 10µm.In absence of NEBD as timing reference anaphase onset was set at 90 minutes (average time from NEBD to anaphase in MMUxMMU zygotes) and the other times calculated accordingly. (B) Initial pro-nuclei distance.

Figure 4. Distribution of paternal and maternal centromeres in control, NocMo and MoNoc treated zygotes. (A) Differential labelling of maternal (magenta) and paternal (cyan) centromeres through distinction of SNPs by fluorescent TALEs. Mitotic spindle is labelled with EB3-mCherry (grey). Representative z-projected images of parental chromosome distribution in untreated, MoNoc and NocMo MMU x MSPS zygotes. Scale bar, 10 µm. (B) Degree of overlap between 3D convex hulls and parental chromosomes for untreated (n=31), MoNoc (n=16), NocMo (n=12) zygotes and embryos with *in silico* randomised distribution (n=40) (see Supplementary Fig. 1 and methods for details).

A

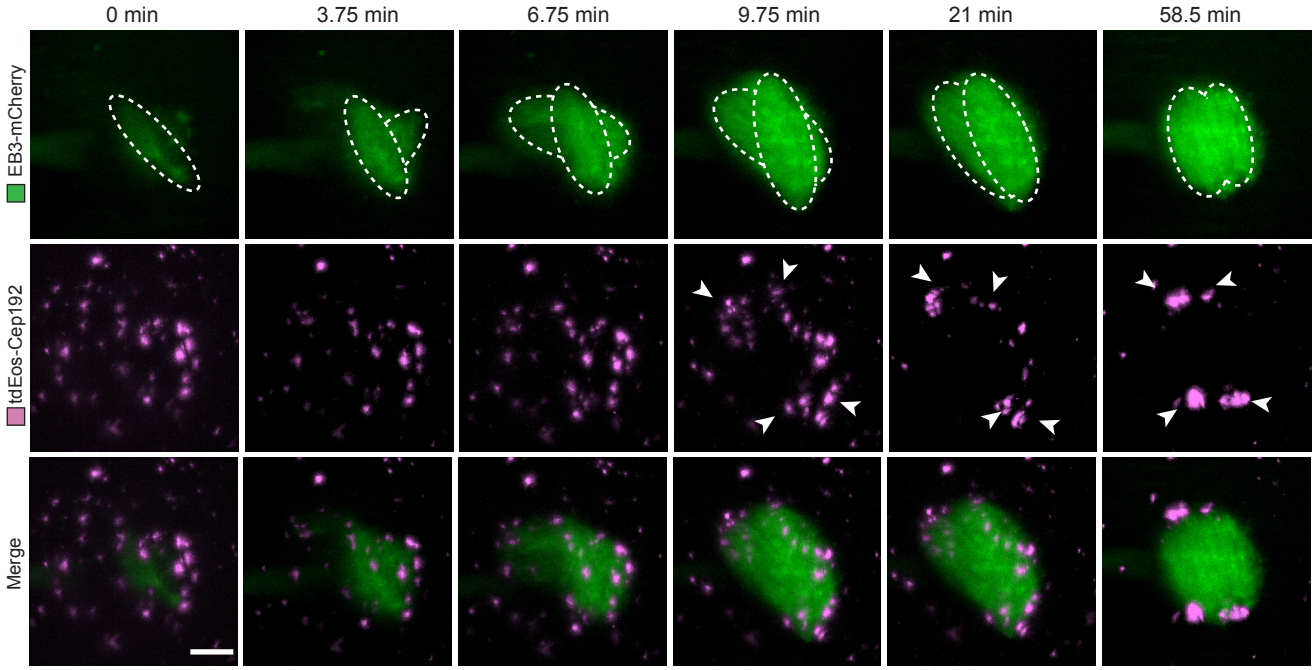
0 min
3.75 min
6.75 min
9.75 min
21 min
58.5 min
EB3-mCherry
tdEos-Cep192
Merge

B

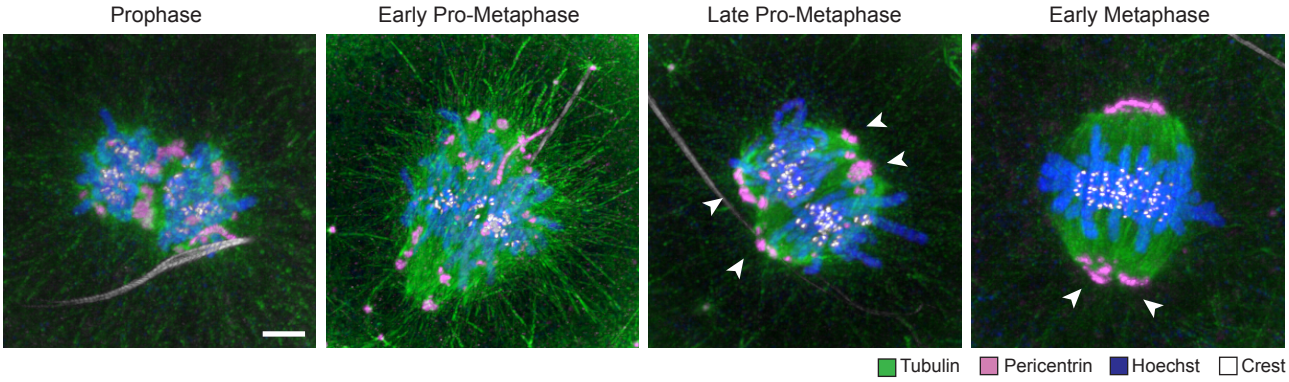
Prophase
Early Pro-Metaphase
Late Pro-Metaphase
Early Metaphase
Tubulin
Pericentrin
Hoechst
Crest

Figure 1

A

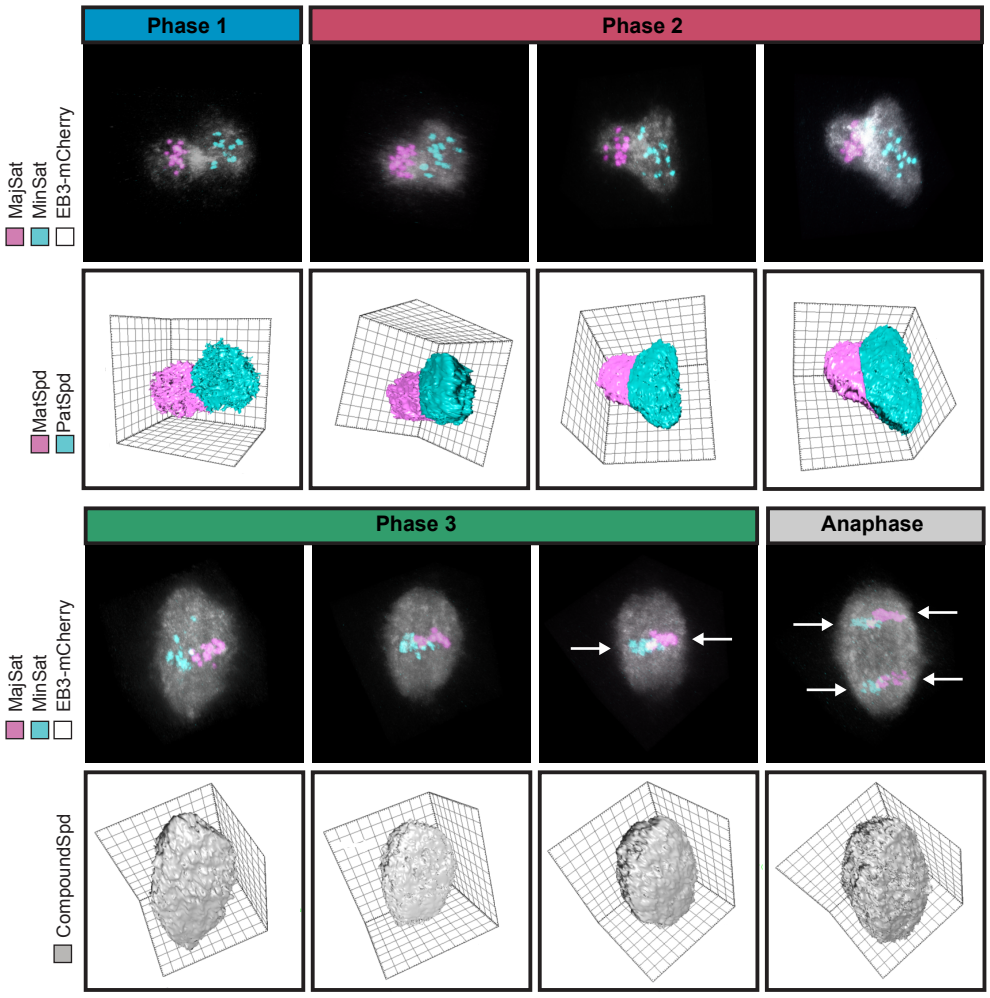

B

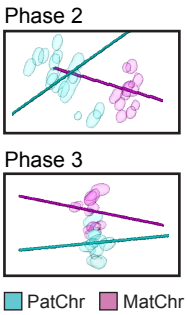

C

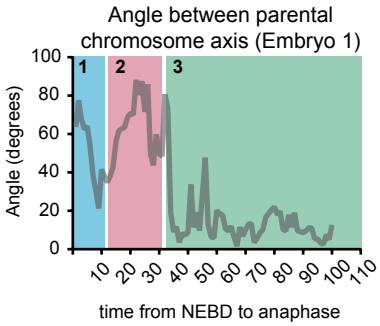

D

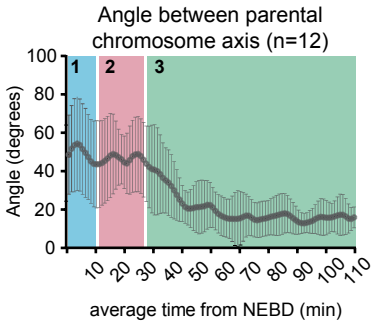

Figure 2

A

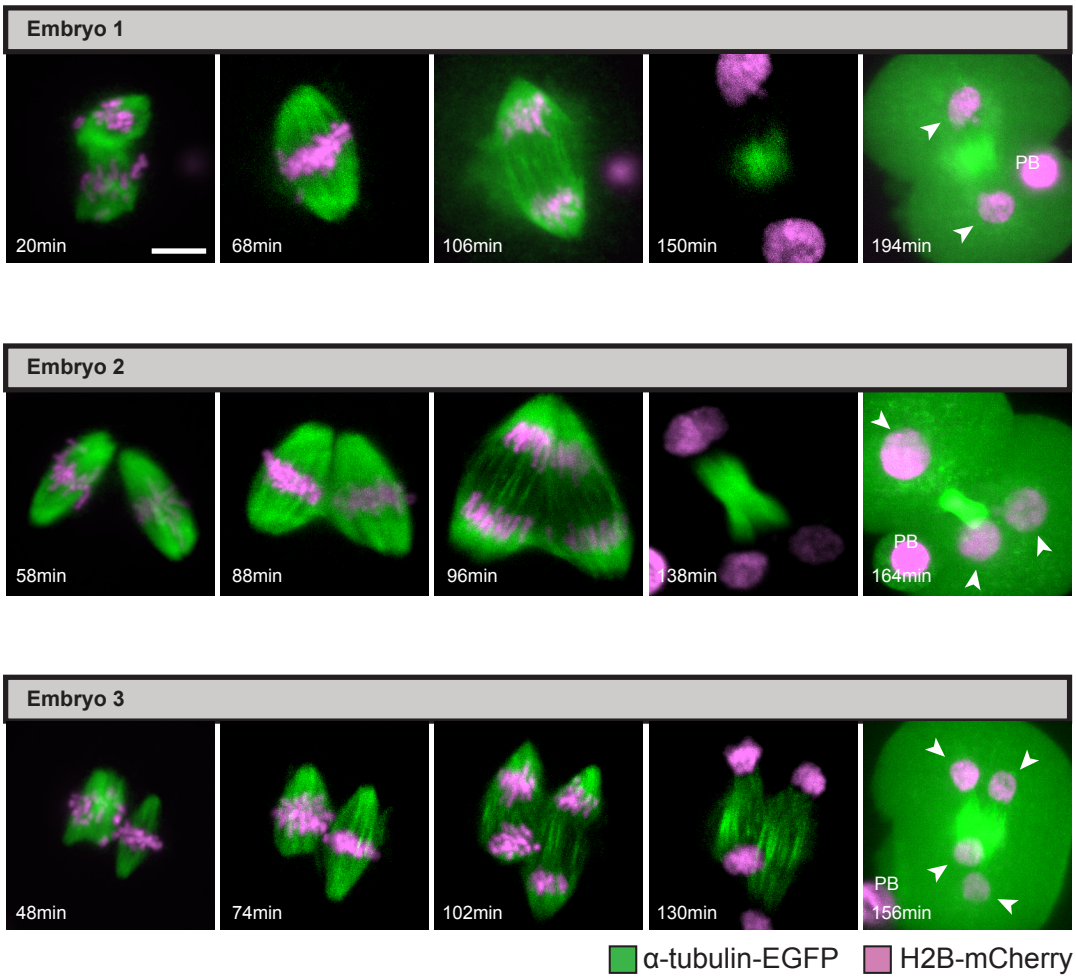
Embryo 1
20min
68min
106min
150min
194min
PB
Embryo 2
58min
88min
96min
138min
164min
PB
Embryo 3
48min
74min
102min
130min
156min
PB
α-tubulin-EGFP
H2B-mCherry

B

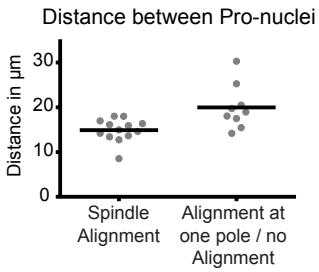
Distance between Pro-nuclei
Distance in µm
30
20
10
0
Spindle Alignment
Alignment at one pole / no Alignment

Figure 3

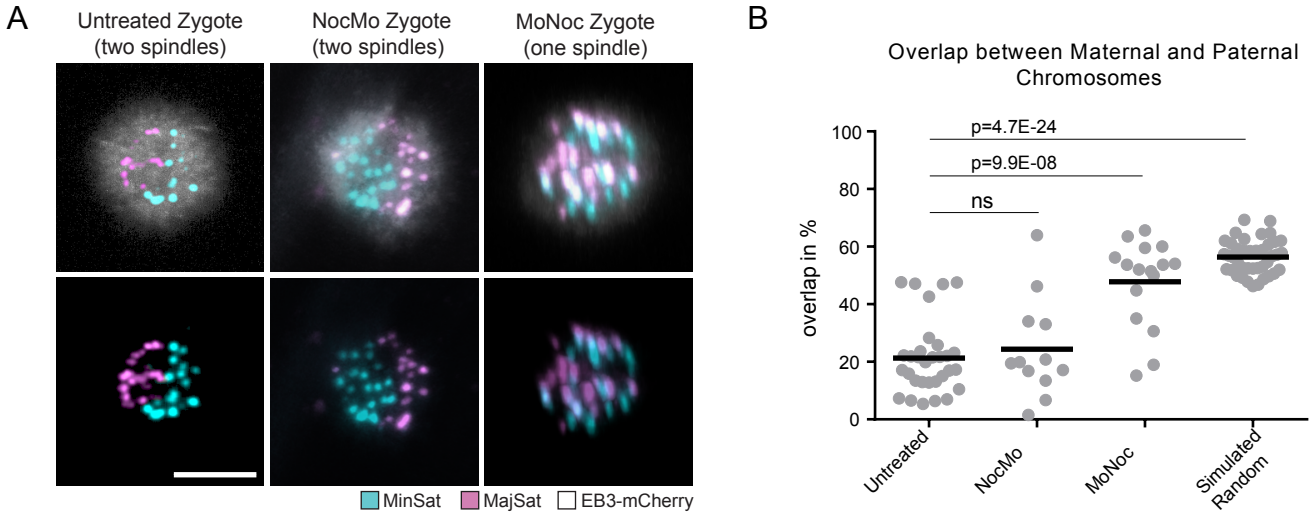
A
Untreated Zygote
(two spindles)
NocMo Zygote
(two spindles)
MoNoc Zygote
(one spindle)
MinSat
MajSat
EB3-mCherry
B
Overlap between Maternal and Paternal Chromosomes
overlap in %
100
80
60
40
20
0
p=4.7E-24
p=9.9E-08
ns
Untreated
NocMo
MoNoc
Simulated Random

Figure 4